Chapter 6

A Proposed Graphene-Gated Semiconductor Terahertz Detector

6.1 Introduction

Research in the THz domain has been picking up the pace over the last few decades. But still, there is a lot of scope for the development of devices in this region. The photosensitivity of the metal-semiconductor field-effect transistor (MESFET) has opened up the possibility of their use for a variety of optoelectronic applications. Of late many works of optically controlled MESFETs based on GaAs material were reported [180]-[189]. A considerable amount of work has been done in the analytical modeling and the fabrication of HgCdTe-based devices operating in short, mid, and long-wavelength IR detectors. Most of the structures studied so far have been diodes [116], [122]-[123], [129], [134], [179]. But there are no studies in devices based on MESFET structures using HgCdTe. Graphene has become the most used material in photodetection applications as it has superior characteristics in a broadband wavelength from UV to THz [155]. Although bandgap tuning is possible and can be operated in the THz region, HgCdTe potential has not been explored yet fully due to a lack of sources. A few works were reported on Graphene/HgCdTe-based detectors [156]-[158]. HgCdTe is a narrow bandgap material having high mobility and a relatively high absorption coefficient. Also, HgCdTe technology is a mature technology. The excellent electrical and optical properties of graphene and equally excellent properties of HgCdTe are combined to form a Schottky contact in a MESFET device [159]. In MESFETs, the current in the channel can be controlled by the gate bias. In the same manner, the current flowing in the channel can also be controlled by incident radiation. In this chapter, analytical modeling of a graphene-gated semiconductor terahertz detector has been proposed. The model proposed takes into consideration the effects of both

photoconductive, as well as photovoltaic effects. The effect of the substrate has not been considered in the present analysis.

6.2 Structure Description

The proposed HgCdTe-GSFET detector structure shown in Fig.6.1 operates at a frequency of 10 THz. The MESFET structure under consideration comprises graphene as a metal gate, a semi-conducting $Hg_{1-x}Cd_xTe$ as a channel, and CdTe as a semi-insulating substrate. The thin graphene layer on the top acts as a semi-transparent material for the incoming THz radiation. The channel is uniformly doped with donor atoms to form an n-$Hg_{1-x}Cd_xTe$. The x-composition of the material is selected such that it absorbs THz radiation at 30 μm wavelength [134], [179]. The THz radiation is assumed to be incident in the vertical direction and the current is assumed to flow in the channel in the horizontal direction from drain to source.

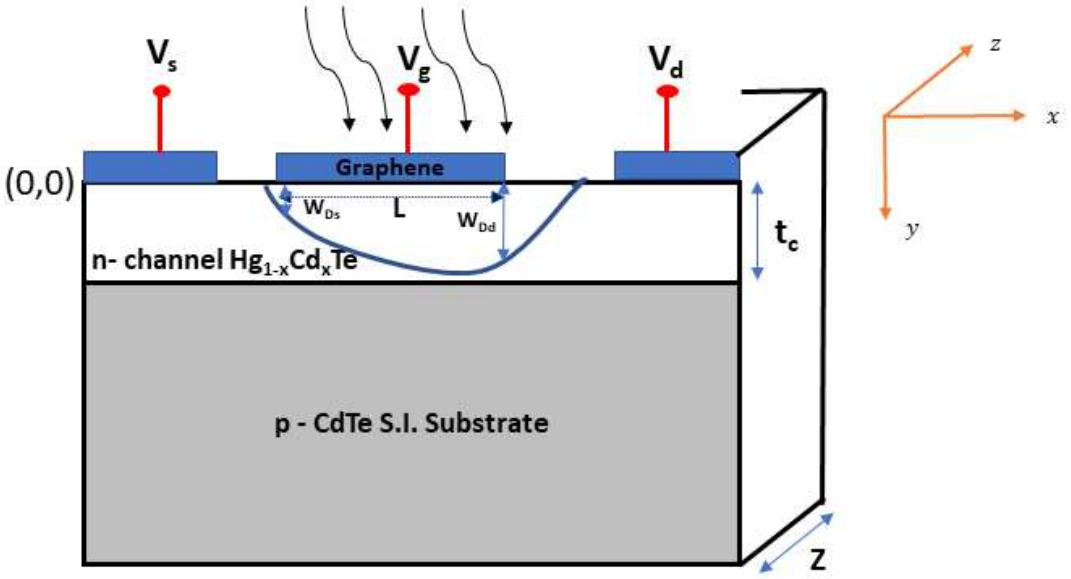

Fig.6.1 Proposed HgCdTe-GSFET Detector

The graphene layer forms a Schottky contact with the $Hg_{1-x}Cd_xTe$ epilayer. A semi-insulating substrate of CdTe material is used upon which the n-type $Hg_{1-x}Cd_xTe$ is supposed to be grown epitaxially. The effect of the substrate has been neglected since it is a wide bandgap material and most of the incident THz radiation is assumed to be absorbed in the channel. Since $Hg_{1-x}Cd_xTe$ is a narrow bandgap material, it is difficult to control the current under dark conditions at room temperature. Hence, to suppress the dark current, an operating temperature of 77 K is considered in the analysis.

6.3 Analytical Modeling

Since there is a mismatch of work functions between graphene and HgCdTe ($\phi_{HgCdTe} < \phi_{Gr}$), a Schottky contact is formed and the expression for the barrier height (ϕ_h) is given as follows [159]

$$\phi_h = \phi_{Gr} - \chi_{HgCdTe} \tag{6.1}$$

where χ_{HgCdTe} is the electron affinity of HgCdTe, ϕ_{Gr} (=4.56 eV) is the work function of graphene.

The built-in potential (V_{bi}) is computed from the formula

$$V_{bi} = \frac{\phi_{Gr} - \phi_{HgCdTe}}{q} \tag{6.2}$$

where ϕ_{HgCdTe} (=4.25 eV) is the work function of HgCdTe (channel).

The thickness of the gate is so small that it is assumed to be transparent to the incident THz radiation. Under illumination, electron-hole pairs are created in the depletion region formed in the epilayer due to the absorption of THz radiation. The excess electrons and holes are

separated by the electric field existing in the depletion region. Poisson's equation in the depletion region under illumination can be written as

$$\frac{d^2V}{dy^2} = -\frac{q}{\epsilon}[N_D + \phi\alpha\tau_L exp(-\alpha y)] \tag{6.3}$$

where ϵ is the permittivity of the channel, and y represents the distance in the region below the gate i.e., the gate depletion region from the Schottky contact.

The photon flux density (ϕ) is given by

$$\phi = \frac{(1-R_m)(1-R_s)P_{opt}}{h\vartheta} \tag{6.4}$$

where P_{opt} is the incident optical power density, R_m is the reflection coefficient for normal incidence at the semi-transparent metal gate and R_m is the reflection coefficient for normal incidence at the metal-epilayer interface.

Under illumination, the excess carriers generated in the channel below the gate affect the minority carrier lifetime. It can be obtained from the expression

$$\frac{\tau_L}{\tau_{Le}} = \frac{n_i}{n_i + \Delta n} \tag{6.5}$$

where τ_{Le} (1 x 10^{-7} s) is the minority carrier lifetime in equilibrium condition, τ_L is the minority carrier lifetime under illuminated conditions.

The number of excess carriers (Δn) generated per unit volume within the semiconductor is given by

$$\Delta n = G_{op}\tau_L = \frac{(1-R_m)(1-R_s)P_{opt}\tau_L}{t_c h\vartheta}(1-\exp(-\alpha t_c)) \tag{6.6}$$

From equations (6.5) and (6.6), the minority carrier lifetime can be obtained as

$$\tau_L = \frac{\left\{1+\frac{4(1-R_m)(1-R_s)}{t_c n_i h\vartheta}P_{opt}\tau_{Le}(1-\exp(-\alpha t_c))\right\}^{1/2}-1}{\frac{2(1-R_m)(1-R_s)}{t_c n_i h\vartheta}P_{opt}(1-\exp(-\alpha t_c))} \tag{6.7}$$

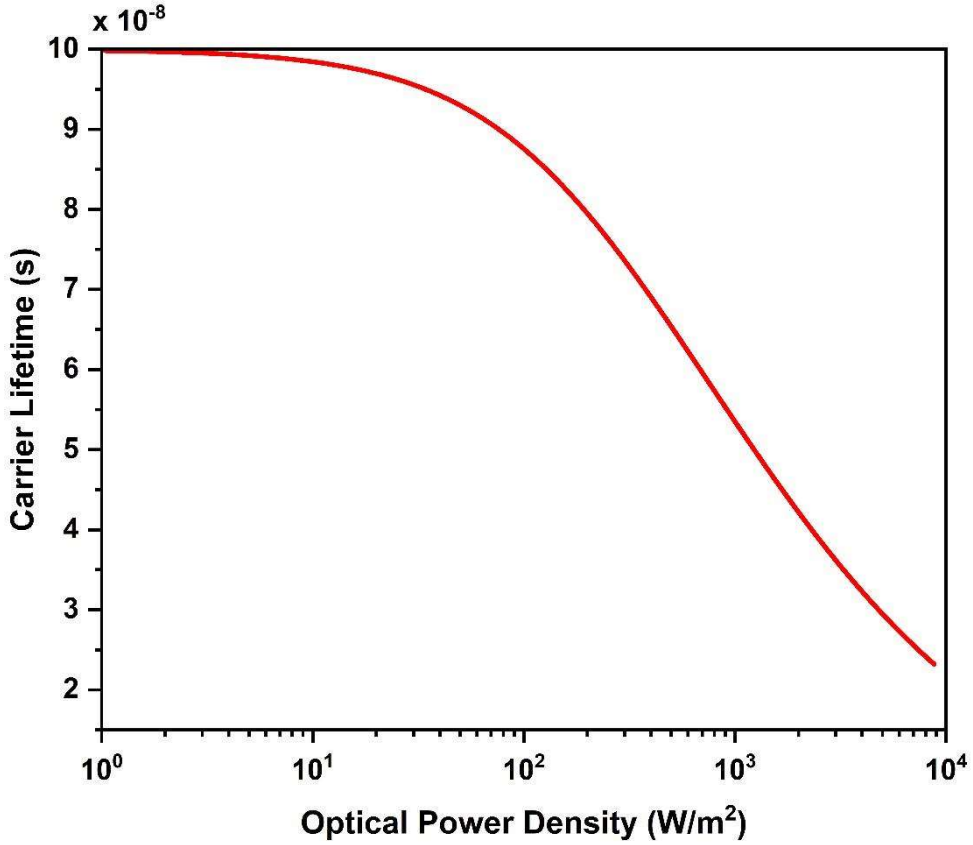

Fig.6.2 Variation of minority carrier lifetime with optical power density

The excess photo-generated carriers in the channel below the gate cause a change in the minority carrier lifetime. It can be seen from Fig.6.2 that the minority carrier lifetime decreases with the increase in the optical power density. As the optical power density is increased, the excess photogenerated carriers increase, and the lifetime is decreased. As the minority carrier lifetime decreases, the recombination is increased, so this will lead to a decrease in the excess carriers. This means that the excess carriers cannot continue increasing with the increase in the optical power density. This decrease in the minority carrier lifetime limits the value of the photovoltage (V_{ph}) developed which will be discussed in the next section.

The Poisson's equation given in equation (6.3) is solved by utilizing the following boundary conditions

$$V(0, W_{Ds}) = V_{bi} + V_{gs} - V_{ph} \tag{6.8}$$

$$V'(W_{Dx}) = 0 \tag{6.9}$$

and

$$V(L, W_{Dd}) = V_d \tag{6.10}$$

where V' represents the first derivative of the potential V with respect to y i.e., the electric field in the depletion region, V_{ph} represents the photovoltage developed across the graphene-HgCdTe Schottky barrier under illumination, V_{gs} represents the gate to source voltage, V_d corresponds to the potential in the channel at the drain end, W_D represents the width of the gate depletion region at any point x from the source towards the drain terminal.

By solving Poisson's equation under the above boundary conditions, the width of the gate depletion region measured from the Schottky junction at any point x in the channel can be obtained as

$$W_D = \left[\frac{2\epsilon\left(V(\mathrm{x}) + V_{bi} + V_{gs} - V_{ph}\right)}{q(N_D + \phi\alpha\tau_L)}\right]^{\frac{1}{2}} \tag{6.11}$$

where $V(\mathrm{x})$ represents the potential in the channel at any point x.

The expressions for the widths of the depletion region at the source end (W_{Ds}) and at the drain end (W_{Dd}) can be expressed as

$$W_{Ds} = \left[\frac{2\epsilon\left(V_s + V_{bi} + V_{gs} - V_{ph}\right)}{q(N_D + \phi\alpha\tau_L)}\right]^{\frac{1}{2}} \tag{6.12}$$

$$W_{Dd} = \left[\frac{2\epsilon\left(V_d + V_{bi} + V_{gs} - V_{ph}\right)}{q(N_D + \phi\alpha\tau_L)}\right]^{\frac{1}{2}} \tag{6.13}$$

where V_s and V_d are the channel potentials at the source end and drain end respectively.

Under the dark condition, it is possible to compute the widths of the depletion region at the source-end and the drain end by putting V_{ph}, and ϕ equal to zero. Since we are interested in finding the effect of illumination on the device, V_{gs} is also assumed to be zero. As the source terminal is grounded, $V(\mathrm{x})$ is assumed to be equal to zero at the source end, and equal to the value of the applied drain voltage at the drain end.

6.3.1 Induced Photovoltage

Mostly the incident THz radiation gets absorbed in the semiconductor region creating excess electron-hole pairs. The excess carriers created cause two effects namely photoconductive

effect and the photovoltaic effect. The carriers created in excess cause a change in the channel's conductivity and the effect is called the photoconductive effect. Also, the generated carriers shorten the longevity of the minority carriers. In addition to the photoconductive effect, the carriers created in excess also cause photovoltage to be formed across the Schottky gate. The photovoltage developed tends to forward bias the Schottky contact which in turn reduces the width of the depletion region thereby increasing the channel's effective thickness. Therefore, it can be concluded that the induced photovoltage causes a change in the channel conductance. The photovoltage of an illuminated Schottky junction is roughly equivalent to the open-circuit voltage in the presence of a large gate bias resistance, and it substantially determines the device's properties under illuminated conditions.

In the presence of illumination, excess carriers will be generated in the gate depletion region and the generation rate decreases exponentially with the vertical direction y in the semiconductor HgCdTe. Therefore, the total photogeneration rate (G_{op}) in $/m^3 s$ can be obtained as [183]

$$G_{op} = 2\,\phi \left\{ \frac{1}{W_{Ds} + W_{Dd}} + \frac{\left(exp(-\alpha W_{Dd}) - exp(-\alpha W_{Ds})\right)}{\alpha(W_{Dd}^2 - W_{Ds}^2)} \right\} \tag{6.14}$$

The photovoltage generated at the Schottky contact can be expressed as [180]

$$V_{ph} = \left(\frac{n_{idl} kT}{q}\right) \ln \left[\frac{q G_{op} \left(\frac{W_{Ds} + W_{Dd}}{2}\right)}{J_{sc}} \right] \tag{6.15}$$

where n_{idl} (=2) represents the ideality factor of the channel, G_{op} represents the generation rate under illumination, and J_{sc} represents the reverse saturation current density.

The reverse saturation current density is given by

$$J_{sc} = A^{**}\, T^2\, exp\left(-\frac{q\phi_h}{kT}\right) \tag{6.16}$$

where A^{**} is the effective Richardson's constant, ϕ_h is the Schottky barrier height.

The photovoltaic effect discussed previously arises from the collection of excess photo-generated carriers in the high electric field in the depletion region which is traverse to the channel. This photovoltage tends to forward bias the Schottky contact and reduces the width of the depletion region. This causes an increase in the effective channel thickness. In other words, the photovoltage modulates the effective channel operating resulting in a change in the channel resistance. The effective channel thickness (t_{eff}) at the drain end under illumination is given as

$$t_{eff} = t_c - \left\{\frac{2\epsilon}{qN_D}\left(V_{bi} + V_{ds} + V_{gs} - V_{ph}\right)\right\}^{1/2} \tag{6.17}$$

where t_c represents the thickness of the channel, V_{ds} is the drain to source voltage.

6.3.2 Current-Voltage Characteristics

In the derivation of the drain current, both the photovoltaic effect and the photoconductive effect have been considered. Due to the illumination, the channel's conductivity is modulated by the excess electron-hole pairs generated. In addition to the photoconductive effect, there is a reduction in the width of the depletion region as a result of photovoltage developed across the Schottky barrier. Therefore, it can be concluded that both the photoconductive and photovoltaic effects cause a change in the conductivity and the channel conductance

respectively under illumination. As a result, a dramatic change in the drain current under the illumination condition flowing in the channel may be observed.

Assuming that the channel is uniformly doped and considering a forward voltage (V_{ph}) to be developed under the Schottky contact under the illumination, the charge stored below the gate is given by

$$Q_n = qN_D(t_c - W_D) \tag{6.18}$$

where Q_n is the charge density.

The expression for the drain current (I_{ds}) has been derived and an approximate expression is obtained by integrating the charge accumulated in the channel per unit area and is given as

$$I_{ds} = \frac{q\mu_n Z}{L}\int_0^{V_{ds}} Q_n dV(x) \tag{6.19}$$

$$I_{ds} \approx \frac{q^2(N_D + \phi\alpha\tau_L)^2}{\epsilon}\frac{\mu_n Z}{L}\left[\frac{t_c W_{Dd}^2}{2} - \frac{W_{Dd}^3}{3} - \frac{t_c W_{Ds}^2}{2} + \frac{W_{Ds}^3}{3}\right] \tag{6.20}$$

where Z is the gate width and L is the gate length.

The expression for the transconductance can be obtained as

$$g_m = \left.\frac{\partial I_{ds}}{\partial V_{gs}}\right|_{V_{ds}=constant} \tag{6.21}$$

That is,

$$g_m \approx q(N_D + \phi\alpha\tau_L)\frac{\mu_n Z}{L}\{W_{Ds} - W_{Dd}\} \tag{6.22}$$

6.4 Results and Discussion

Numerical computations have been performed for the HgCdTe-GSFET detector at a temperature of 77 K. The doping of the channel has been assumed to be uniform with a concentration of $1 \times 10^{22}\ /m^3$. The graphene and the epilayer of HgCdTe form a Schottky contact. Since the material for the channel is a narrow bandgap material and the substrate is CdTe which is a wide bandgap material, most of the incident THz radiation gets absorbed in the channel on the assumption that the gate is a semi-transparent material. Therefore, the effect of the substrate has been neglected. The parameters used in the computation are listed in Table 6.1. Most of the HgCdTe material parameters used here are taken from [107].

Table 6.1 Parameters used in the calculation at a temperature of 77 K

Parameter	**Value**	**References**
x-composition	0.175325	[134]
Channel thickness (t_c)	0.35 µm	(assumed)
Gate Length (L)	1 µm	(assumed)
Gate Width (Z)	10 µm	(assumed)
Absorption Coefficient (α) of $Hg_{1-x}Cd_xTe$	1.46478 x 10^5 /m	[134]
Energy Bandgap (E_g) of $Hg_{1-x}Cd_xTe$	41.4 meV	[134]
Wavelength of Interest (λ)	30 µm	[134]
Intrinsic Carrier Concentration of $Hg_{1-x}Cd_xTe$ (n_i)	1.2485 x 10^{21} /m^3	[134]
Electron Affinity (χ) of $Hg_{1-x}Cd_xTe$	4.2639 eV	[134]
Electron Mobility (μ_n) of $Hg_{1-x}Cd_xTe$	19.9517 m^2/Vs	[134]
Barrier Height (ϕ_h)	0.2961 eV	[159]
Minority Carrier Lifetime (τ_L)	1 x 10^{-8} s	[107]
Built-in Potential (V_{bi})	0.31 V	[159]

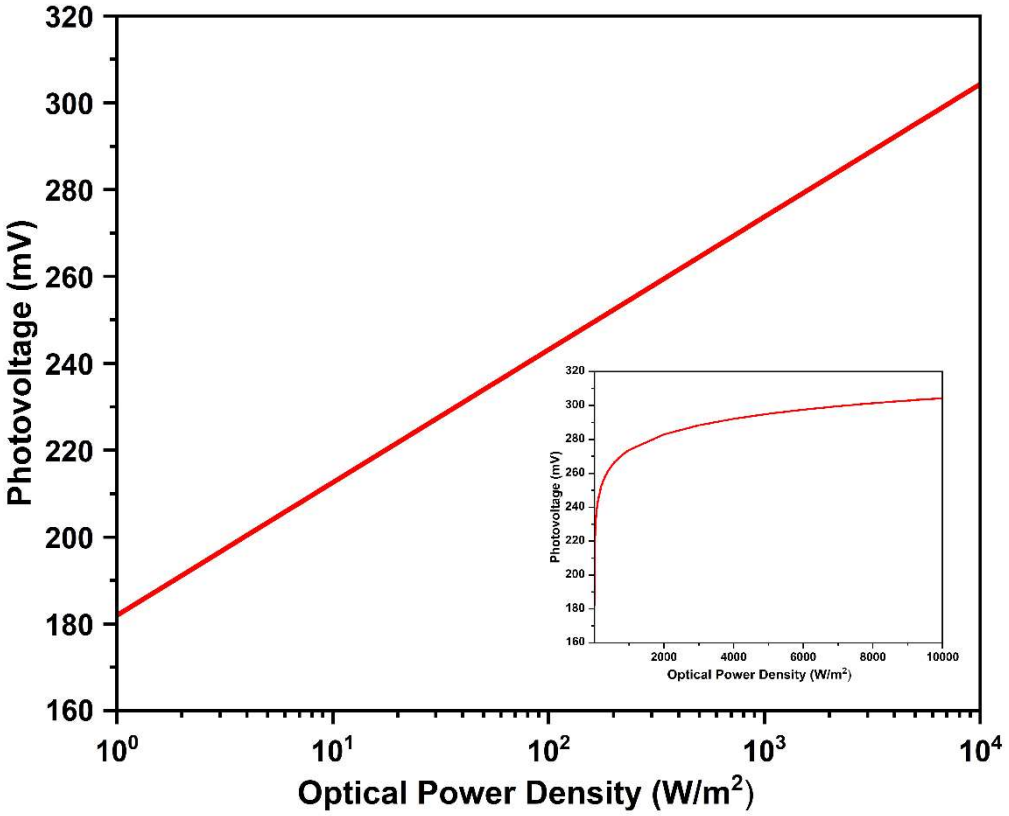

Fig.6.3 Variation of photovoltage under different incident optical power densities

Fig.6.3 shows the variation of the photovoltage developed across the graphene-HgCdTe Schottky barrier with the incident THz radiation of optical power densities. It is seen that the photovoltage increases non-linearly with the incident optical power. The photovoltage, V_{ph} cannot increase indefinitely with the increase in the optical power since the minority carrier lifetime decreases due to an increased number of excess carriers with the increase in optical power density. This decrease in minority carrier lifetime under illumination limits the value of optically generated carrier rate which in turn causes the photovoltage to saturate at a very high value of power density. Optical power density has been taken in the log scale. It can be seen in Fig.6.3 that the photovoltage increases with the increase in the optical power density initially but tends to saturate for higher values of optical power densities.

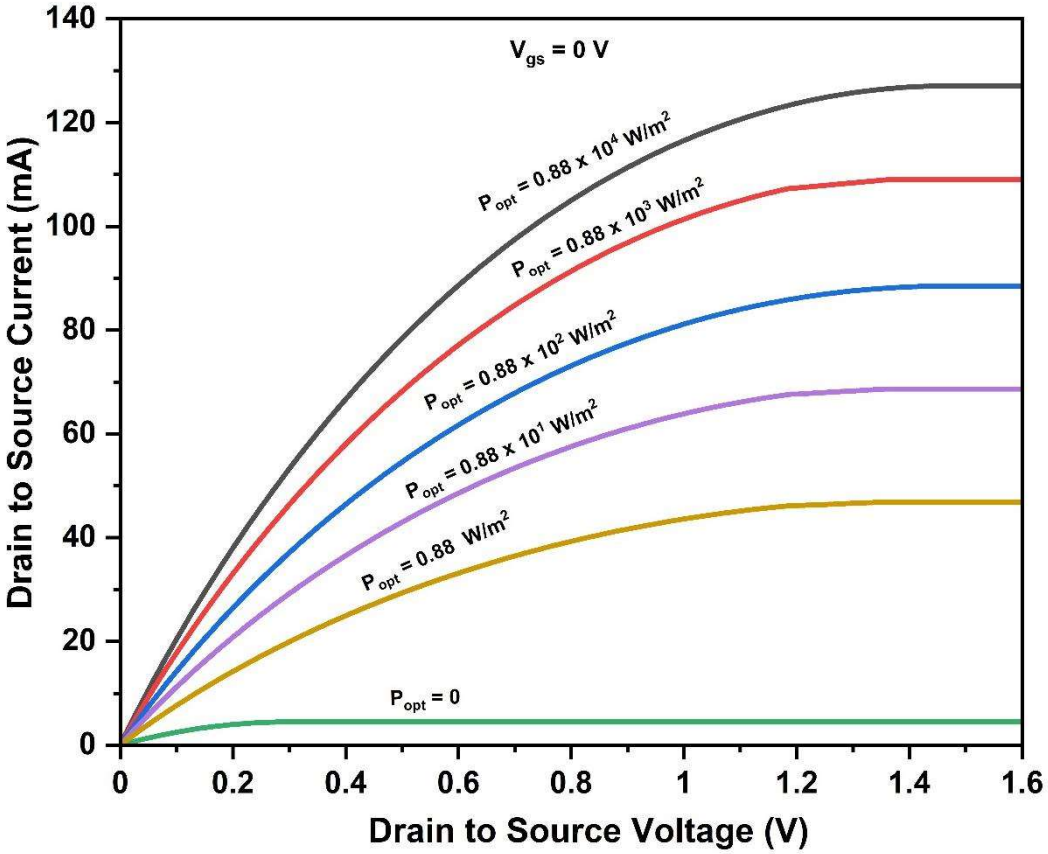

Fig.6.4 Drain characteristics of the HgCdTe-GSFET detector under dark and various optical power densities

It is evident from the drain characteristics shown in Fig.6.4 that in the presence of illumination, under the combined influence of the photoconductive effect and the photovoltaic effect, there is a tremendous increase in the drain current in comparison to that in the dark condition. It shows that the higher the optical power density the larger the drain current. Optical power density of $P_{opt} = 0.88 \times 10^4\ W/m^2$ is used for the analysis. The higher values of optical power densities are not considered in the analysis as the drain current saturates.

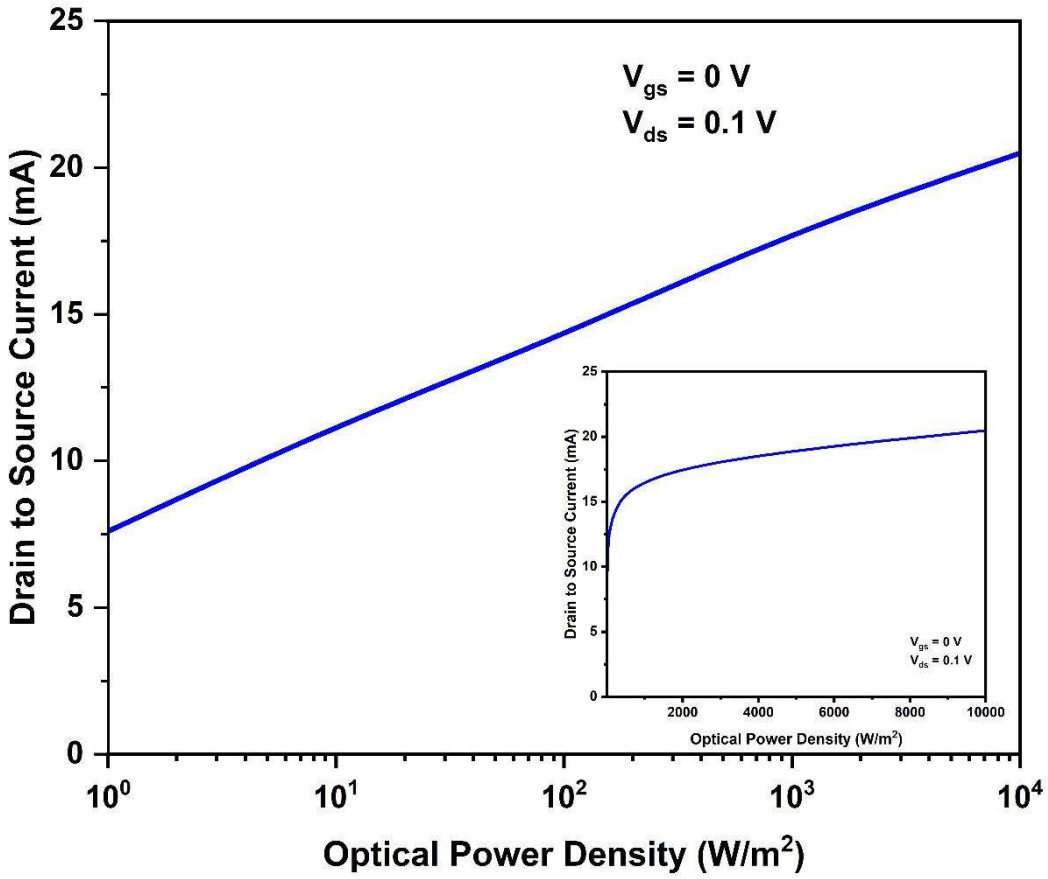

Fig.6.5 Variation of drain to source current with optical power density

Fig.6.5 shows the variation of drain to source current with the optical power density. The value of current increases with the increase in power density. The increase in the value of photovoltage and the excess carriers in the channel is the main reason behind this increase of the drain current. But at higher optical power densities, as explained previously the limitations of the minority carrier lifetime on the photovoltage causes the current to saturate.

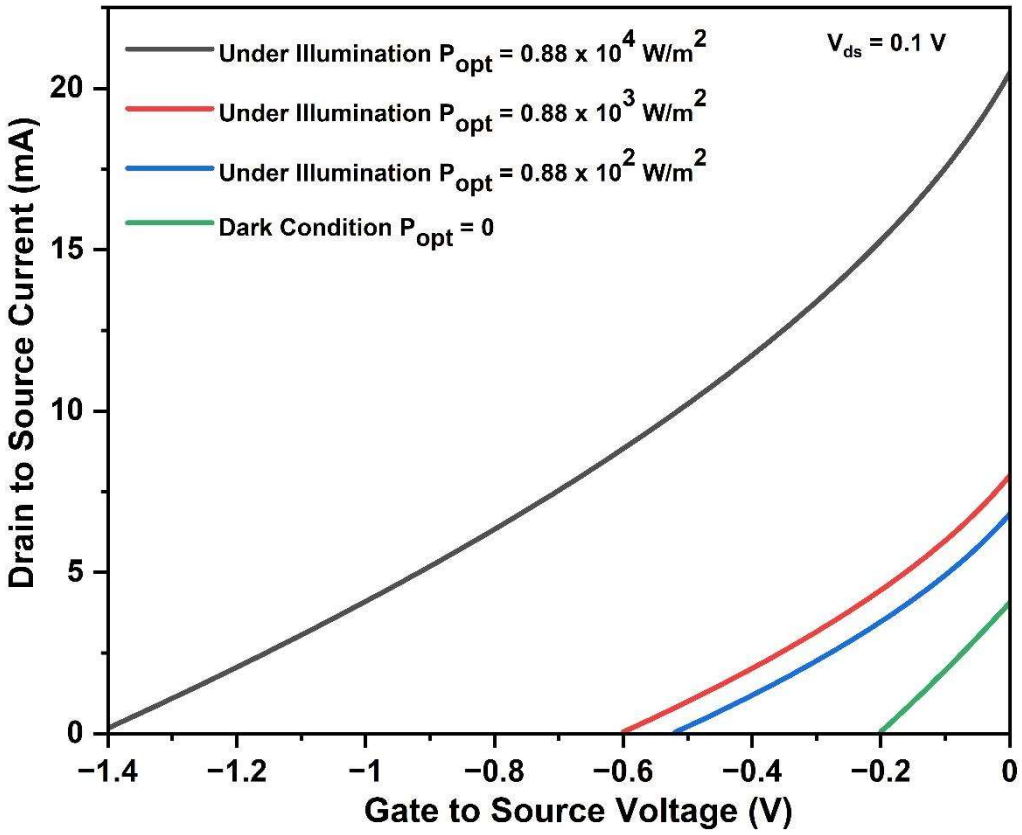

Fig.6.6 Transfer characteristics of the HgCdTe-GSFET under dark and illumination conditions

It is evident from the transfer characteristics shown in Fig.6.6 that in the presence of illumination under various optical power densities, there is a change in the pinch-off voltage relative to its values in the dark condition.

We can observe that the pinch-off voltage under illumination condition is found to be $V_p = -1.4\ V$ for an optical power density of $P_{opt} = 0.88 \text{ x } 10^4 W/m^2$.

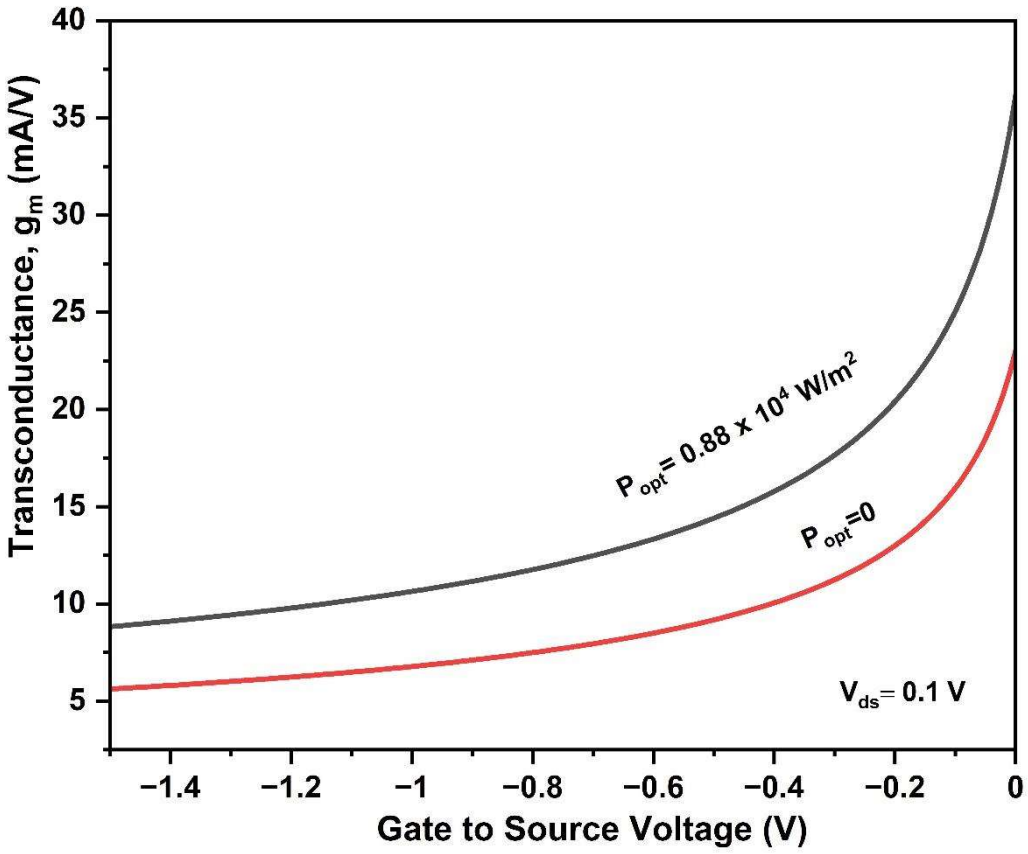

Fig.6.7 Variation of transconductance versus applied gate-to-source voltage

Fig.6.7 shows the variation of transconductance with the applied gate-to-source voltage. It is seen that the transconductance decreases with the increase in the gate-to-source voltage under a constant $V_{ds} = 0.1\ V$ and an optical power density of $P_{opt} = 0.88 \text{ x } 10^4 W/m^2$.

Also, the optical gain of the GSFET considered is computed using the expression

$$\text{Optical gain} = \frac{I_{illum} - I_{dark}}{I_{dark}} \tag{6.23}$$

where I_{illum} is the current in the device under illumination and I_{dark} is the current under dark condition. The optical gain is found to be 27.11. The variation of optical gains under different optical power densities have been listed in Table 6.2.

Table 6.2 Comparison of optical gain for various incident optical power densities

	Incident Optical Power Density (W/m^2)	Optical Gain
Proposed Device	$P_{opt} = 0.88$	09.37
	$P_{opt} = 0.88 \times 10^1$	14.19
	$P_{opt} = 0.88 \times 10^2$	18.57
	$P_{opt} = 0.88 \times 10^3$	23.11
	$P_{opt} = 0.88 \times 10^4$	27.11

6.5 Conclusion

The model presented in this chapter opens a new possibility of exploring the potential of a graphene-based MESFET built with a narrow bandgap material as a promising candidate for the development of future generation THz detectors. The graphene layer has been used to provide a Schottky contact to serve as a semi-transparent metal gate. The GSFET can be operated as THz radiation-controlled device which can be operated with or without a gate voltage. The attractive feature of the device is that in the absence of an applied gate voltage, the THz radiation can control the current-voltage (I_D-V_D) characteristics of the device. The device operates at an optical power density of the order of 0.88 x 10^4 W/m^2. It exhibits a very low dark current of the order of 4.52 mA. It also possesses a good optical gain of 27.11. The high-speed feature of a Schottky-barrier field-effect transistor is expected to make the GSFET device especially attractive for the application of a detector in THz communication systems.